Received March 29, 2019, accepted April 10, 2019, date of publication April 15, 2019, date of current version April 26, 2019.

Digital Object Identifier 10.1109/ACCESS.2019.2911176

GFDM Based Wireless Powered Communication for Cooperative Relay System

ZHENYU NA[1], (Member, IEEE), JIAQI LV[1], MENGSHU ZHANG[1], BAO PENG[2], MUDI XIONG[1], AND MINGXIANG GUAN[2]

[1]School of Information Science and Technology, Dalian Maritime University, Dalian 116026, China
[2]School of Electronic Communication Technology, Shenzhen Institute of Information Technology, Shenzhen 518000, China

Corresponding authors: Jiaqi Lv (lvjiaqi@dlmu.edu.cn) and Bao Peng (pengb@sziit.edu.cn)

This work was supported in part by the National Natural Science Foundations of China under Grant 61301131, in part by the Fundamental Research Funds for the Central Universities under Grant 3132016347 and Grant 3132019214, in part by the Guangdong Province Higher Vocational Colleges and Schools Pearl River Scholar Funded Scheme, and in part by the Project of Shenzhen Science and Technology Innovation Committee under Grant JCYJ20170817114522834.

ABSTRACT Green and sustainable communications are crucial for cellular devices and the Internet of Things (IoT) devices in the fifth generation (5G) mobile communication system. Wireless-powered communication (WPC) provides a successful technical paradigm to support wireless information transmission for mobile devices by using harvested radio-frequency (RF) energy. In the meantime, non-orthogonal multicarrier transmission techniques, typically represented by the generalized frequency-division multiplexing (GFDM), can not only enhance spectrum efficiency but also improve the flexibility of resource allocation due to its fine-granularity sub-block. In this paper, a GFDM-based cooperative relay system model is proposed to improve the quality of experience of the cell-edge user. Specifically, the system is composed of one source node, one destination node (cell-edge user), and one relay node. The source node transmits a signal to the destination node and the relay node. The relay node performs information transmission and power transfer to the destination node by using different GFDM sub-block sets. The destination node combines the signals from the source node and relay node. In order to maximize the information rate at the destination node subject to the minimum harvested energy, a joint sub-block, sub-block power, and subslot allocation-based WPC scheme is proposed. To solve the non-convex optimization problem, an iterative algorithm is proposed and its effectiveness is validated by simulations. The simulation results demonstrate that the GFDM-based WPC scheme outperforms the orthogonal frequency-division multiplexing (OFDM), and the subslot optimization can significantly increase the information rate at the destination node.

INDEX TERMS 5G, wireless powered communication, generalized frequency division multiplexing, cooperative relay, optimization.

I. INTRODUCTION

Compared with the Fourth Generation (4G) wireless communication networks, the Fifth Generation (5G) pays more attention to Gbps-level data transmission, massive Machine-Type Communications (MTC), high spectrum efficiency and consistent quality of user experience [1]–[6].

The exponential increase of data rate requires high energy consumption that drastically shortens the battery life of mobile devices [7]–[10]. As the effective energy supplement method to extend the battery life of energy-constrained devices, Energy Harvesting (EH) technique has drawn unprecedented attention from academia and industry [11]–[13]. Different from natural energy sources, since Radio Frequency (RF) signal carries information and energy simultaneously, it can serve as self-sustainable and controllable energy source for wireless Power Transfer (PT) to mobile devices [14]–[17]. For devices of MTC and Human-Type Communications (HTC) in 5G networks, Information Transmission (IT) always contradicts with battery energy storage. By means of EH from RF signal, a good tradeoff between IT and battery energy storage can be achieved. Just based on the idea, the concept of Wireless Powered Communication (WPC) is proposed [18]–[21], which is a successful technical paradigm to support simultaneous wireless IT and PT for mobile devices. Therefore, WPC is indispensable for

The associate editor coordinating the review of this manuscript and approving it for publication was Qilian Liang.

both MTC and HTC because mobile devices can receive or transmit information by using the harvested energy to extend network lifetime.

As another vision of 5G, higher spectrum utilization is a challenging task. Traditionally, the Orthogonal Frequency Division Multiplexing (OFDM) is adopted by the Long-Term Evolution (LTE) as one of the key physical-layer techniques [22]. However, the surge of needs of Augmented Reality (AR), ultra-high definition mobile broadband, intelligent logistics, automatic driving and mission-critical application makes OFDM incompetent in 5G application scenarios mainly due to its insufficient spectrum utilization. Breaking the limitation of orthogonality between subcarriers, the Generalized Frequency Division Multiplexing (GFDM), which is one of the non-orthogonal multicarrier transmission schemes, can significantly improve spectrum efficiency [23]. Deriving from OFDM, GFDM not only inherits many merits of OFDM, but also has its own unique technical advantages including low Peak to Average Power Ratio (PAPR), loose synchronization and low Out-of-Band (OoB) radiation. Especially, the data block of GFDM has a two-dimensional structure in time and frequency domains that makes resource allocation more flexible and accurate. Since GFDM is originally designed oriented to 5G networks, it also supports MTC and HTC.

Over the past few years, WPC and its applications to OFDM systems have been extensively investigated to improve the quality of user experience [12], [22], [24]–[27]. [12] studied the downlink resource allocation in a multi-user OFDM system to maximum the sum information rate of all users subject to the minimum harvested energy, and provided a research paradigm for resource allocation in the multi-user and multi-subcarrier system. A secure WPC scheme was proposed for OFDM system to transmit information and transfer energy [25]. By optimizing the cyclic prefix length, time-switching and power-splitting parameters and the power allocation ratio, the average secrecy rate is maximized subject to the average energy transfer rate at the legitimate receiver. In [26], an OFDM based WPC model for IoT scenarios was proposed in which each device decodes information and harvests energy simultaneously over the downlink, and then transmits signals over the uplink. The optimization objective is to maximize the sum information rate over the uplink subject to the target sum information rate over the downlink. A broadband WPC system was proposed in which the subband sets are divided into two parts for two independent frequency domain signals based on two complementary spectrum marker vectors: one for IT and the other one for PT [27]. The system throughput is maximized by jointly optimizing subband sets and subband power subject to the constraints of energy and interference. From the analyses above, the present research on multi-carrier based WPC mainly focuses on OFDM. Different from the most work, [22] paid attention to non-orthogonal multi-carrier based WPC. In [22], the authors proposed a joint subcarrier and subsymbol allocation scheme in GFDM based WPC system for the first time. By utilizing the two-dimensional block structure of GFDM, the optimization problem to maximize the sum information rate over the downlink by jointly optimizing subcarrier and subsymbol allocation, power allocation and power splitting ratio subject to the total transmit power and harvested energy is investigated.

Considering the case when a user is located at cell edge, cooperative relay can be applied to extend wireless network coverage and meliorate the quality of user experience. There are plenty of research achievements on cooperative relay transmissions [28]–[31]. In [28], an Energy Efficient (EE) resource allocation scheme was investigated in OFDM bidirectional relay system. Joint subcarrier and power allocation, and relay node selection were optimized subject to the minimum system throughput. The novel optimal EE power allocation scheme was derived to minimize the overall transmit power consumption. Reference [29] investigated OFDM based cooperative transmission model for Wireless Sensor Networks (WSNs) in smart cities. In the model, a Relay Sensor Node (RSN) divides the received signals into two groups for EH and IT in the first phase, respectively. In the second phase, RSN forwards information to the Destination Sensor Node (DSN) based on the harvested energy. The optimization objective is to maximize the information rate at Source Sensor Node (SSN) by jointly optimizing subcarrier grouping, subcarrier pairing and power allocation under power constraints. A WPC scheme for multi-user OFDM based relay system was proposed in [30]. To maximize the system sum information rate, power allocation, subcarrier allocation and incremental policy are jointly optimized, subject to the power constraint. In order to reduce the computational complexity, the multi-dimensional degrees of freedom are sequentially and iteratively derived. In [31], a WPC backscatter communication network deployed with a power beacon station was proposed. Each backscatter radio harvests energy to sustain battery-less transmissions, some other radios serve as relays to realize cooperative transmission. The WPC and relay strategies were formulated in order to maximize the system throughput.

According to the literature reviews above, it can be seen that there is no work on GFDM based WPC for cooperative relay system. Therefore, a GFDM based cooperative relay system model is proposed in this paper to improve quality of experience and extend battery life for cell-edge user. The main contributions of this paper are summarized as follows.

- A GFDM based cooperative relay system model is proposed for the first time. On one hand, compared with OFDM, GFDM supports higher spectrum efficiency and information rate. On the other hand, the relay node in the model performs IT and PT simultaneously so that the quality of experience and battery life for cell-edge user can be significantly improved. To the best of our knowledge, this is the first time to propose a model combined cooperative relay transmission with GFDM for WPC.

- A joint sub-block, sub-block power and subslot allocations based WPC scheme is proposed. The two-dimensional structure of GFDM data defined in both time and frequency domains makes resource allocation more flexible than the one-dimensional structure of OFDM data only defined in frequency domain. In GFDM, a time-frequency resource unit corresponding to a certain subcarrier and subsymbol is defined as a sub-block. Based on the concept of sub-block, power allocation can be performed at a fine granularity so that channel conditions can be utilized sufficiently. Besides, the traditional cooperative transmission adopts two equal subslots, but the optimal system performance is often corresponding to two different subslots. Therefore, the proposed joint WPC scheme is of significance.
- An iterative algorithm is designed to solve the proposed optimization problem. According to system model and WPC scheme, an optimization problem to maximize the information rate at cell-edge user is formulated under several constraints. Because the optimization problem is non-convex, Lagrange duality method is applied and a low-complexity iterative algorithm is designed to sequentially and iteratively obtain the optimal solution to the optimization problem.

The remaining of this paper is organized as follows. In section II, the GFDM based cooperative relay system model is proposed, as well as the principle of GFDM is introduced. The optimization problem is formulated in section III. In section IV, the iterative algorithm based on the Lagrange duality method is designed. The simulation results and performance discussions are presented in section V. Finally, section VI concludes this paper.

II. SYSTEM MODEL

When a user is located at cell edge, the long propagation distance, severe fading and strong interference from adjacent cells would deteriorate the quality of received signal. Cooperative relay transmission can effectively expand wireless network coverage and improve the signal reception of cell-edge user. In this paper, a GFDM based cooperative relay system model which consists of one source node (Base Station, BS), one destination node (cell-edge user, represented by T) and one relay node (represented by R) is proposed, as depicted in Fig.1. The BS transmits signal to the cell-edge user T and relay R. The relay R performs IT and PT to the cell-edge user T by using different GFDM sub-block sets. The cell-edge user T combines the signals from the BS and relay R.

In GFDM based communication system, the binary data stream is firstly Quadrature Amplitude Modulation (QAM) modulated, and then mapped into a data vector $\vec{d}$ consisting of KM elements, where K and M are numbers of subcarriers and subsymbols, respectively. After serial-to-parallel conversion, the vector $\vec{d}$ is reshaped into a $K \times M$ data vector $\vec{X}$ as follows.

$$X = \begin{bmatrix} x_{0,0} & \cdots & x_{0,M-1} \\ \vdots & \ddots & \vdots \\ x_{K-1,0} & \cdots & x_{K-1,M-1} \end{bmatrix} \tag{1}$$

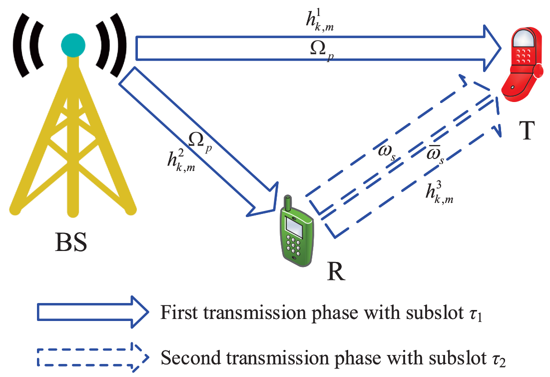

FIGURE 1. GFDM based cooperative relay system model.

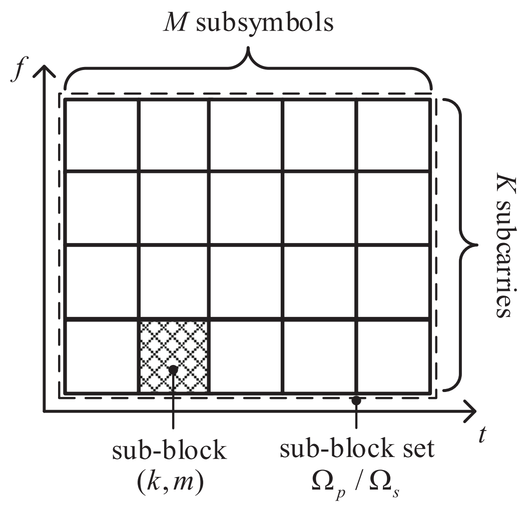

FIGURE 2. GFDM block structure.

where $x_{k,m}$ denotes the transmitted data of BS on the k-th subcarrier and in the m-th subsymbol.

Thus, the GFDM modulated data of BS and R are transmitted over the two-dimensional block as depicted in Fig.2. The time-frequency resource unit on the k-th subcarrier and in the m-th subsymbol is defined as sub-block (k, m) [22], $1 \leq k \leq K, 1 \leq m \leq M$. In particular, GFDM turns into OFDM when $M = 1$ [32]. The sub-block sets of BS and R are respectively denoted by $\mathbf{\Omega}_p$ and $\mathbf{\Omega}_s$, where $\mathbf{\Omega}_p = \mathbf{\Omega}_s$ and $|\mathbf{\Omega}_p| = |\mathbf{\Omega}_s| = KM$.

The transmission process from BS to T is divided into two phases. In the first transmission phase with subslot τ_1, the data over sub-block set $\mathbf{\Omega}_p$ is transmitted from BS to T and R, respectively. In the second transmission phase with subslot τ_2, R divides $\mathbf{\Omega}_s$ into two subsets $\boldsymbol{\omega}_s$ and $\bar{\boldsymbol{\omega}}_s$ to simultaneously perform IT and PT to T, where $\boldsymbol{\omega}_s + \bar{\boldsymbol{\omega}}_s = \mathbf{\Omega}_s$ and $\boldsymbol{\omega}_s \cap \bar{\boldsymbol{\omega}}_s = \varnothing$. For simplicity, the transmission slot is set to 1s, and the constraint of $\tau_1 + \tau_2 = 1$ must be satisfied. On one hand, R combines $\boldsymbol{\omega}_s$ with a subset $\boldsymbol{\omega}_p \subseteq \mathbf{\Omega}_p$ to transmit information to T based on Decode-and-Forward (DF) protocol [3], [5]. Let us suppose $\boldsymbol{\omega}_s = \boldsymbol{\omega}_p$ that means the two subsets are correspondingly paired. On the other hand, R utilizes $\bar{\boldsymbol{\omega}}_s$ to transmit power to T.

The relationship of summation for different sub-block sets $\boldsymbol{\Omega}_p$, $\boldsymbol{\Omega}_s$, $\boldsymbol{\omega}_s$ and $\bar{\boldsymbol{\omega}}_s$ is given as follows.

$$\sum_{(k,m)\in\boldsymbol{\Omega}_p} = \sum_{k=1}^{K}\sum_{m=1}^{M} = \sum_{(k,m)\in\boldsymbol{\Omega}_s} = \sum_{(k,m)\in\boldsymbol{\omega}_s} + \sum_{(k,m)\in\bar{\boldsymbol{\omega}}_s} \tag{2}$$

The channel coefficients of BS → T link, BS → R link and R → T link over sub-block (k, m) are denoted by $h^i_{k,m}$, $i = 1, 2, 3$. The channel power gains are defined as $\gamma^i_{k,m} \triangleq |h^i_{k,m}|^2$, $i = 1, 2, 3$. For convenience, slow fading is considered so that the channel power gain over each link is constant within a transmission phase and known at the transmitter. All noise items at the receivers over BS → T link, BS → R link and R → T link are modeled as Additive White Gaussian Noise (AWGN) random variables with zero mean and variance $\sigma^2 = 1$. The transmit data sent by BS over sub-block (k, m) is denoted by $x_{k,m}$, and the corresponding transmit power is $p^{BS}_{k,m}$. Similarly, the transmit power of the data sent by R over sub-block (k, m) is denoted by $p^R_{k,m}$. The total transmit power of BS and R are P_t and P_s, respectively. The maximum and minimum power allocated to sub-block (k, m) are P_{max} and P_{min}, respectively. This can be seen as the spectral masks in multi-subcarrier system to meet the requirement of practical power limits and the neighboring user interference constraint [33]. The water-filling algorithm is applied to allocate power to each sub-block at BS. The required minimum harvested energy at T is E_T.

III. PROBLEM FORMULATION

The transmission process from BS to T is divided into two phases whose subslots are τ_1 and τ_2, respectively. The constraint of subslots of two-phase transmission is given by

$$\tau_1 + \tau_2 = 1, \quad \tau_1, \tau_2 > 0 \tag{3}$$

In the first transmission phase, the data over sub-block set $\boldsymbol{\Omega}_p$ is transmitted from BS to T and R, respectively. The received signals at T and R over the sub-block (k, m) are respectively given by

$$y^{T1}_{k,m} = \sqrt{p^{BS}_{k,m}} h^1_{k,m} x_{k,m} + n^T_{k,m} \tag{4}$$

$$y^{R}_{k,m} = \sqrt{p^{BS}_{k,m}} h^2_{k,m} x_{k,m} + n^R_{k,m} \tag{5}$$

where $n^T_{k,m}$ and $n^R_{k,m}$ are AWGN items at T and R, respectively. Particularly, $p^{BS}_{k,m} = \left(\frac{1}{\lambda} - \frac{1}{\gamma^1_{k,m}}\right)^+$, $(a)^+ = \max(a, 0)$, and $\frac{1}{\lambda}$ is the water-filing line obtained for the total power constraint $\sum_{k=1}^{K}\sum_{m=1}^{M} p^{BS}_{k,m} = P_t$ based on the water-filling algorithm. Thus, the sum information rates over sub-block set $\boldsymbol{\Omega}_p$ associated with the decoded $x_{k,m}$ from $y^{T1}_{k,m}$ and $y^R_{k,m}$ are respectively expressed by

$$R^{T1} = \sum_{(k,m)\in\boldsymbol{\Omega}_p} \tau_1 \log_2\left(1 + \frac{p^{BS}_{k,m}\gamma^1_{k,m}}{\sigma^2}\right) \tag{6}$$

$$R^{R} = \sum_{(k,m)\in\boldsymbol{\Omega}_p} \tau_1 \log_2\left(1 + \frac{p^{BS}_{k,m}\gamma^2_{k,m}}{\sigma^2}\right) \tag{7}$$

In the second transmission phase, the sub-block set $\boldsymbol{\Omega}_s$ is divided into two subsets $\boldsymbol{\omega}_s$ and $\bar{\boldsymbol{\omega}}_s$. The former performs IT for T by using DF protocol, while the latter performs PT. Given the energy conversion efficiency η, the harvested energy at T over the sub-block set $\bar{\boldsymbol{\omega}}_s$ is expressed by

$$E = \sum_{(k,m)\in\bar{\boldsymbol{\omega}}_s} \tau_2\eta\left(p^R_{k,m}\gamma^3_{k,m} + \sigma^2\right) \tag{8}$$

When it comes to IT, the received signal at T over the sub-block (k, m) is given by

$$y^{T2}_{k,m} = \sqrt{p^R_{k,m}} h^3_{k,m} x_{k,m} + n^T_{k,m} + \tilde{n}^R_{k,m} \tag{9}$$

where $\tilde{n}^R_{k,m}$ is AWGN item derived from RF-to-baseband conversion and decoding operation by using DF processing. Then, the sum rate at T over the sub-block set $\boldsymbol{\omega}_s$ is expressed by

$$R^{T2} = \sum_{(k,m)\in\boldsymbol{\omega}_s} \tau_2 \log_2\left(1 + \frac{p^R_{k,m}\gamma^3_{k,m}}{2\sigma^2}\right) \tag{10}$$

Based on DF protocol [34], [35], the information rate at T through two-phase cooperative transmission is given by

$$R_{tot} = \min[R^R, R^{T1} + R^{T2}] \tag{11}$$

The optimization objective is to maximize the information rate at T by jointly optimizing the sub-block transmit power, sub-block set and transmission subslot allocations under the constraints of total transmit power, minimum harvested energy and transmission slot. The transmission subslot vector is denoted as $\boldsymbol{\tau} = [\tau_1, \tau_2]$. The sub-block transmit power vector is denoted as $\boldsymbol{p} = \{p^R_{k,m}\}$. The corresponding optimization problem is formulated as follows.

$$\begin{aligned}
&\max_{\boldsymbol{p},\boldsymbol{\omega}_s,\boldsymbol{\tau}} R_{tot} = \min[R^R, R^{PR1} + R^{PR2}]\\
&s.t. \sum_{(k,m)\in\boldsymbol{\omega}_s} p^R_{k,m} + \sum_{(k,m)\in\bar{\boldsymbol{\omega}}_s} p^R_{k,m} \le P_s, \quad \forall k, m\\
&\qquad p^R_{k,m} \ge 0, \quad \forall k, m\\
&\qquad E \ge E_T\\
&\qquad \tau_1 + \tau_2 = 1, \quad \tau_1, \quad \tau_2 > 0
\end{aligned} \tag{12}$$

IV. OPTIMAL SOLUTION

In this section, we focus on solving the joint optimization problem (12). It is worth noting that the objective function of problem (12) is the minimum of R^R and $R^{T1} + R^{T2}$. If $R^R \le R^{T1} + R^{T2}$, the objective function is simplified as $\max_{\boldsymbol{p},\boldsymbol{\omega}_s,\boldsymbol{\tau}} R^R$ that is only related to $\boldsymbol{\tau}$ without involving $\boldsymbol{p}$ and $\boldsymbol{\omega}_s$. Therefore, the condition that makes problem (12) meaningful is $R^R \geq R^{T1} + R^{T2}$. Three variables are defined to simplify the problem formulation as follows.

$$A_{k,m} \triangleq \log_2\left(1 + p_{k,m}^{BS}\gamma_{k,m}^2\right)$$
$$B_{k,m} \triangleq \log_2\left(1 + p_{k,m}^{BS}\gamma_{k,m}^1\right)$$
$$C_{k,m} \triangleq \log_2\left(1 + \frac{p_{k,m}^{R}\gamma_{k,m}^3}{2}\right) \tag{13}$$

Substituting (2),(13), $\tau_2 = 1 - \tau_1$ and $\sigma^2 = 1$ into problem (12), the joint optimization problem can be reformulated as

$$\begin{aligned}
\max_{\boldsymbol{p},\boldsymbol{\omega}_s,\tau_2} R_{tot} &= \sum_{k=1}^{K}\sum_{m=1}^{M}(1-\tau_2)B_{k,m} + \sum_{(k,m)\in\boldsymbol{\omega}_s}\tau_2 C_{k,m} \\
s.t. \ &\sum_{(k,m)\in\boldsymbol{\omega}_s} p_{k,m}^R + \sum_{(k,m)\in\bar{\boldsymbol{\omega}}_s} p_{k,m}^R \leq P_s, \quad \forall k,m \\
&\sum_{(k,m)\in\bar{\boldsymbol{\omega}}_s} \tau_2\eta\left(p_{k,m}^R\gamma_{k,m}^3 + 1\right) \geq E_T \\
&\sum_{k=1}^{K}\sum_{m=1}^{M}(1-\tau_2)(A_{k,m}-B_{k,m}) \geq \sum_{(k,m)\in\boldsymbol{\omega}_s}\tau_2 C_{k,m} \\
&0 < \tau_2 < 1
\end{aligned} \tag{14}$$

The optimization problem is non-convex because the discrete decision variables $\boldsymbol{\omega}_s$ makes the objective function and constraints non-convex. Since to obtain the optimal solution directly suffers high computational complexity, the Lagrange duality method is adopted and an iterative algorithm is proposed in the following subsections to solve the non-convex optimization problem efficiently [36]. Firstly, the dual variables are updated for the given $\boldsymbol{p}$, $\boldsymbol{\omega}_s$ and τ_2. Secondly, $\boldsymbol{p}$, $\boldsymbol{\omega}_s$ and τ_2 are updated for the given dual variables. The two steps are alternately performed until a target accuracy is satisfied.

A. OPTIMIZING DUAL VARIABLES

The Lagrangian function is given by

$$\begin{aligned}
&\mathcal{L}(\boldsymbol{p},\boldsymbol{\omega}_s,\tau_2) \\
&= \sum_{k=1}^{K}\sum_{m=1}^{M}(1-\tau_2)B_{k,m} + \sum_{(k,m)\in\boldsymbol{\omega}_s}\tau_2 C_{k,m} \\
&\quad + \mu_1\left(P_s - \sum_{(k,m)\in\boldsymbol{\omega}_s} p_{k,m}^R - \sum_{(k,m)\in\bar{\boldsymbol{\omega}}_s} p_{k,m}^R\right) \\
&\quad + \mu_2\left(\sum_{(k,m)\in\bar{\boldsymbol{\omega}}_s}\tau_2\eta\left(p_{k,m}^R\gamma_{k,m}^3 + 1\right) - E_T\right) \\
&\quad + \mu_3\left(\sum_{k=1}^{K}\sum_{m=1}^{M}(1-\tau_2)(A_{k,m}-B_{k,m}) - \sum_{(k,m)\in\boldsymbol{\omega}_s}\tau_2 C_{k,m}\right)
\end{aligned} \tag{15}$$

where $\boldsymbol{\mu} = [\mu_1, \mu_2, \mu_3]$ is the dual variable vector subject to the three constraints in the problem (14). The Lagrange dual function is defined as

$$g(\mu) = \max_{\boldsymbol{p},\boldsymbol{\omega}_s,\tau_2} \mathcal{L}(\boldsymbol{p},\boldsymbol{\omega}_s,\tau_2) \tag{16}$$

The dual problem equivalent to the problem (14) is then written as

$$\min_{\boldsymbol{\mu}} g(\boldsymbol{\mu}), \quad \boldsymbol{\mu} \geq 0 \tag{17}$$

After obtaining the optimal transmit power $\boldsymbol{p}$, sub-block set $\boldsymbol{\omega}_s$ and transmission subslot τ_2 for the problem (14) to maximize $\mathcal{L}(\boldsymbol{p},\boldsymbol{\omega}_s,\tau_2)$, the convex dual function $g(\boldsymbol{\mu})$ can be obtained according to (16). Then, the convex dual problem in (17) can be solved based on the subgradient method [37]. The subgradients of dual variables are given as follows

$$\begin{aligned}
\Delta\mu_1 &= P_s - \sum_{(k,m)\in\boldsymbol{\omega}_s} p_{k,m}^R - \sum_{(k,m)\in\bar{\boldsymbol{\omega}}_s} p_{k,m}^R \\
\Delta\mu_2 &= \sum_{(k,m)\in\bar{\boldsymbol{\omega}}_s}\tau_2\eta\left(p_{k,m}^R\gamma_{k,m}^3 + 1\right) - E_T \\
\Delta\mu_3 &= \sum_{k=1}^{K}\sum_{m=1}^{M}(1-\tau_2)(A_{k,m}-B_{k,m}) - \sum_{(k,m)\in\boldsymbol{\omega}_s}\tau_2 C_{k,m}
\end{aligned} \tag{18}$$

Define the subgradients vector $\Delta\boldsymbol{\mu} = [\Delta\mu_1, \Delta\mu_2, \Delta\mu_3]$, the dual variables can be updated in the negative subgradient direction to get the optimal dual variables with guaranteed convergence [33]:

$$\boldsymbol{\mu}' = \boldsymbol{\mu} - t\Delta\boldsymbol{\mu} \tag{19}$$

where $\boldsymbol{t} = [t_1, t_2, t_3]$ is the non-negative step size vector.

B. OPTIMIZAING RESOURCE ALLOCATION WITH GIVEN DUAL VARIABLES

In this subsection, $\boldsymbol{p}$, $\boldsymbol{\omega}_s$ and τ_2 are optimized in three steps. Firstly, $\boldsymbol{p}$ is optimized for the fixed $\boldsymbol{\omega}_s$ and τ_2. Then, τ_2 is optimized for the optimal $\boldsymbol{p}^*$ and the fixed $\boldsymbol{\omega}_s$. Finally, $\boldsymbol{\omega}_s$ is updated based on the optimal $\boldsymbol{p}^*$ and τ_2^*.

1) Optimizing $\boldsymbol{p}$ for the fixed $\boldsymbol{\omega}_s$ and τ_2: For the fixed $\boldsymbol{\omega}_s$ and τ_2, the partial derivatives of Lagrangian function in (15) with respect to $p_{k,m}^R$, $(k,m) \in \boldsymbol{\omega}_s$ and $p_{k,m}^R$, $(k,m) \in \bar{\boldsymbol{\omega}}_s$ are respectively given as follows.

$$\begin{aligned}
\frac{\partial\mathcal{L}}{\partial p_{k,m}^R} &= \frac{2\tau_2(1-\mu_3)\gamma_{k,m}^3}{\left(2 + p_{k,m}^R\gamma_{k,m}^3\right)\ln 2} - \mu_1, \quad (k,m) \in \boldsymbol{\omega}_s \\
\frac{\partial\mathcal{L}}{\partial p_{k,m}^R} &= \mu_2\tau\eta\gamma_{k,m}^3 - \mu_1, \quad (k,m) \in \bar{\boldsymbol{\omega}}_s
\end{aligned} \tag{20}$$

The Karush-Kuhn-Tucker (KKT) conditions are applied to set the partial derivatives to zero. Thus, the optimal solution to $p_{k,m}^R$, $(k,m) \in \boldsymbol{\omega}_s$ and $p_{k,m}^R$, $(k,m) \in \bar{\boldsymbol{\omega}}_s$ are respectively obtained as follows.

$$p_{k,m}^{R*} = \min\left(P_{max}, \left(\frac{2\tau(1-\mu_3)}{\mu_1 \ln 2} - \frac{2}{\gamma_{k,m}^3}\right)\right)^+,$$
$$(k,m) \in \boldsymbol{\omega}_s$$
$$p_{k,m}^{R*} = \begin{cases} lrP_{max}, & \mu_2\tau\eta\gamma_{k,m}^3 - \mu_1 \geq 0 \\ P_{min}, & \mu_2\tau\eta\gamma_{k,m}^3 - \mu_1 < 0 \end{cases} \quad (k,m) \in \bar{\boldsymbol{\omega}}_s \tag{21}$$

2) Optimizing τ_2 for the optimal $\boldsymbol{p}^*$ and the fixed $\boldsymbol{\omega}_s$: There is a compromise between the objective function and the third constraint in the problem (14). The condition that maximizes the objective function is given as follows.

$$\sum_{k=1}^{K}\sum_{m=1}^{M}(1-\tau_2)(A_{k,m} - B_{k,m}) = \sum_{(k,m)\in\boldsymbol{\omega}_s} \tau_2 C_{k,m} \tag{22}$$

Substituting (21) into (22), the optimal solution to transmission subslot τ_2 is calculated by

$$\tau_2^* = \frac{\sum_{k=1}^{K}\sum_{m=1}^{M}(A_{k,m} - B_{k,m})}{\sum_{k=1}^{K}\sum_{m=1}^{M}(A_{k,m} - B_{k,m}) + \sum_{(k,m)\in\boldsymbol{\omega}_s} C_{k,m}^*} \tag{23}$$

3) Optimizing $\boldsymbol{\omega}_s$ for the optimal $\boldsymbol{p}^*$ and τ_2^*: Substituting (2), (21) and (23) into (15), the Lagrangian function can be rewritten as

$$\begin{aligned} \mathcal{L}(\boldsymbol{p}, \boldsymbol{\omega}_s, \tau_2) = &\sum_{(k,m)\in\boldsymbol{\omega}_s} F_{k,m}^* \\ &+ \sum_{k=1}^{K}\sum_{m=1}^{M}(1-\tau_2^*)B_{k,m} \\ &+ \mu_1\left(P_s - \sum_{k=1}^{K}\sum_{m=1}^{M} p_{k,m}^{R*}\right) \\ &+ \mu_2\left(\sum_{k=1}^{K}\sum_{m=1}^{M}\tau_2^*\eta\left(p_{k,m}^{R*}\gamma_{k,m}^3 + 1\right) - E_T\right) \\ &+ \mu_3\sum_{k=1}^{K}\sum_{m=1}^{M}(1-\tau_2^*)(A_{k,m} - B_{k,m}) \end{aligned} \tag{24}$$

where

$$F_{k,m}^* = \tau_2^*\left(C_{k,m}^* - \mu_2\eta\left(p_{k,m}^{R*}\gamma_{k,m}^3 + 1\right) - \mu_3 C_{k,m}^*\right) \tag{25}$$

Since only the first term on the right-hand side of (24) involves $\boldsymbol{\omega}_s$, the optimal sub-block set $\boldsymbol{\omega}_s^*$ can be obtained by

$$\boldsymbol{\omega}_s^* = \arg\max_{\boldsymbol{\omega}_s} \sum_{(k,m)\in\boldsymbol{\omega}_s} F_{k,m}^* \tag{26}$$

where all the sub-blocks (k,m) which make $F_{k,m}^*$ positive constitute $\boldsymbol{\omega}_s$.

The proposed iterative algorithm for the optimization problem (12) according to above three steps is shown in Table 1.

TABLE 1. The proposed iterative algorithm for the optimization problem (12).

1. Initialize $\boldsymbol{\omega}_s$, τ_2 and non-negative dual variables in vector $\boldsymbol{\mu}$. Calculate
   $\{p_{k,m}^{BS}\}$ according to water-filling algorithm.
2. **repeat**
   A) Calculate $\{p_{k,m}^{R}\}$ according to (21).
   B) Calculate τ_2 according to (23).
   C) All the sub-blocks (k,m) which makes $F_{k,m}^*$ in (25) positive constitute $\boldsymbol{\omega}_s$.
   D) Calculate the subgradients according to (18).
   E) Update dual variables in vector $\boldsymbol{\mu}$ according to (19).
3. **until** all subgradients in vector $\Delta\boldsymbol{\mu}$ meet the prescribed accuracy.

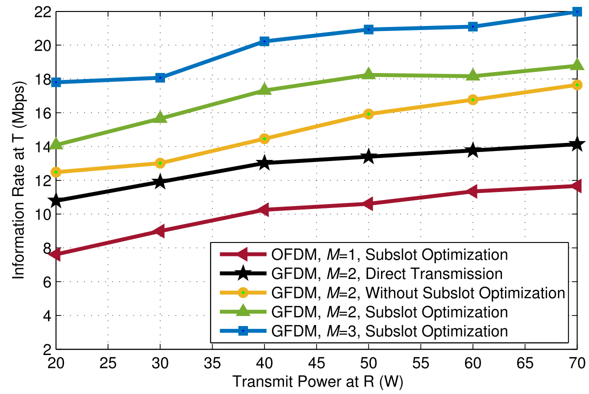

FIGURE 3. Information rate at T versus transmit power at R.

V. SIMULATION RESULTS AND DISCUSSIONS

In this section, simulation results are presented to demonstrate the performance of the proposed GFDM based WPC scheme for the cooperative relay system in terms of information rate and the harvested energy at the cell-edge user T.

In simulations, the independent Rayleigh fading channel with unit mean is considered for BS → T link, BS → R link and R → T link. The bandwidth of GFDM modulated system is set to 1MHz, which is divided into $K = 8$ subcarriers. The total transmit power of BS $P_t = 40$W, the noise variance $\sigma^2 = 1$, the energy conversion efficiency $\eta = 0.8$ and the step size of subgradients is set to $t_1 = t_2 = t_3 = 0.001$.

Fig.3 demonstrates the information rate at the cell-edge user T versus the transmit power of the relay R in the case of fixed harvested energy $E_T = 5$J. As mentioned before, GFDM reduces to OFDM when the number of subsymbols is equal to 1 ($M = 1$). It can be seen that information rate at T increases with the increase of transmit power at R. This can be interpreted as follows. With the increase of transmit power at R, the average power of sub-blocks used for IT and PT increases. On one hand, the minimum harvested energy E_T can be achieved by fewer sub-blocks. On the other hand, the power of sub-blocks used for IT becomes larger leading to higher information rate at T.

In order to demonstrate the performance advantage of GFDM over that of OFDM, the information rate of GFDM and OFDM based systems is simulated in Fig.3. Under the same condition of optimized subslot, the information rate at

T for OFDM system ($M = 1$), GFDM system ($M = 2$) and GFDM system ($M = 3$) is demonstrated in Fig.3 with brown line, green line and blue line, respectively. Two phenomena can be observed. First, all the cases based on GFDM system outperform that based on OFDM. Second, the information rate at T increases with the increase of the number of sub-symbols. These phenomena can be explained as follows. Compared with OFDM, since the two-dimensional structure of GFDM data block increases the flexibility of resource allocation in time domain, the fine granularity of sub-block in time and frequency domains can make full use of channel conditions leading to more desirable resource allocation matching to user requirement.

For the GFDM system, under the same condition of the same number of subsymbols ($M = 2$), three cases are taken into consideration including case (1): direct transmission, case (2): without subslot optimization, and case (3): subslot optimization. Considering the transmission slot is 1, the two subslots in case (2) is 0.5s and 0.5s, respectively. There are also two phenomena in Fig.3 that should be noticed. First, compared with case (1), the information rate for cases (2) and (3) is higher than the former mainly because cooperative diversity contributes to the improvement of information rate for the cell-edge user T. Second, compared with case (2), case (3) provides higher information rate mainly because subslot optimization can determine the optimal subslot allocation for two transmission phases and achieve best performance.

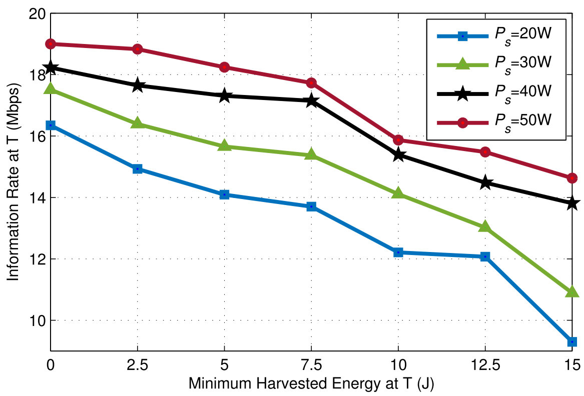

FIGURE 4. Information rate versus minimum harvested energy at T.

Fig.4 demonstrates the information rate versus the minimum harvested energy at the cell-edge user T for different values of transmit power P_s at the relay R. For a given P_s, it is obvious that the information rate decreases with the increase of the minimum harvested energy. Specifically, the increase of the minimum harvested energy means that more sub-blocks and more power are used for PT to T, and less power is utilized for IT resulting in the decrease of information rate. For a given minimum harvested energy, since the proportion of sub-blocks and power used for PT decreases with the increase of transmit power P_s, the average power of sub-blocks used for IT increases leading to the increase of information rate at T.

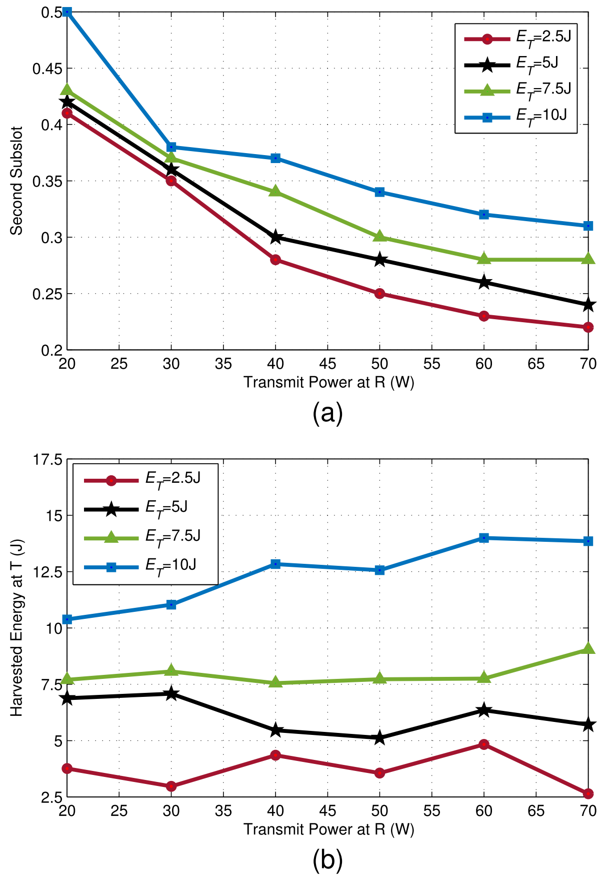

FIGURE 5. Subslot optimization and harvested energy at T versus transmit power at R.

Given $M = 2$, Fig.5a demonstrates the optimized subslot τ_2 versus the transmit power at the relay R, and Fig.5b shows the harvested energy at the cell-edge user T versus the transmit power at the relay R. It can be seen from Fig.3 that, with the increase of transmit power at R, the average power of sub-blocks used for IT and PT increases for a given E_T. Thus, the required subslot τ_2 of the second transmission phase to achieve the minimum harvested energy decreases. It is obvious that, for a given transmit power at R, the increase of the minimum harvested energy leads to the increase of subslot τ_2. It can be seen from Fig.5b that the proposed algorithm can guarantee the target harvested energy E_T for different values of transmit power at R. Thus, the cell-edge user T can achieve higher information rate when the transmit power at the relay R increases.

Given $M = 2$, $P_s = 40$W and $E_T = 10$J, Fig.6 demonstrates the power allocated to different sub-blocks versus channel condition. Notice that the m-th sybsymbol includes all the sub-blocks (k, m), $k = 1, \ldots, 8$, $m = 1, 2$. The subfigure (a) and (b) is corresponding to the first and the second subsymbol, respectively. As shown in Fig.6, power is not allocated to the sub-blocks with poor channel conditions mainly because the objective to improve the information rate forces power to be allocated to the sub-blocks with good channel conditions. Then, since the channel conditions of

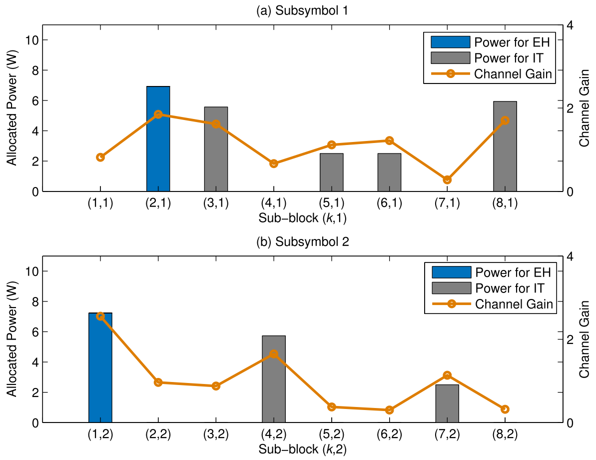

FIGURE 6. Power over different sub-blocks versus channel condition.

sub-block (2,1) and (1,2) are the best, more power is allocated to achieve the target harvested energy. Besides, it can be observed that power allocated for IT is more than that for PT mainly because the target harvested energy is relatively small, and only few power and sub-blocks are required.

VI. CONCLUSION

Wireless powered communication can support simultaneous information transmission and energy transfer for mobile devices. As two promising techniques in 5G communications, GFDM can effectively enhance spectrum efficiency and support flexible resource allocation, while cooperative relay transmission can significantly improve the reception quality of cell-edge user. In this paper, a GFDM based cooperative relay system model to support WPC for cell-edge user is proposed. By using DF protocol, the relay node simultaneously forwards information and transfer power over sub-blocks to the cell-edge user. The optimization objective is to maximize the information rate at the cell-edge user by jointly optimizing the sub-block transmit power, sub-block set and transmission subslot allocations subject to total transmit power, minimum harvested energy and transmission slot. The Lagrange duality method and proposed iterative algorithm are used to obtain the solution to the optimization problem. Simulation results reveal the following conclusions. Firstly, the cooperative relay system based on GFDM outperforms that based on OFDM mainly because the two-dimensional time-frequency structure of GFDM data block makes resource allocated at a fine granularity in time and frequency domains. Thus, power allocation over sub-blocks can accurately adapt to the channel conditions and achieve higher information rate. Secondly, subslot optimization contributes to the improvement of information rate at the cell-edge user mainly because the two-stage transmission process is optimally balanced. Finally, the proposed iterative algorithm can effectively obtain the optimal solution to the optimization problem and flexibly allocate resource according to the channel conditions.

REFERENCES

[1] X. Liu, M. Jia, X. Zhang, and W. Lu, "A novel multi-channel Internet of Things based on dynamic spectrum sharing in 5G communication," *IEEE Internet Things J.*, to be published.

[2] D. Zhai, R. Zhang, J. Du, Z. Ding, and F. R. Yu, "Simultaneous wireless information and power transfer at 5G new frequencies: Channel measurement and network design," *IEEE J. Sel. Areas Commun.*, vol. 37, no. 1, pp. 171–186, Jan. 2019.

[3] M. Jia, Z. Yin, D. Li, Q. Guo, and X. Gu, "Toward improved offloading efficiency of data transmission in the IoT-cloud by leveraging secure truncating OFDM," *IEEE Internet Things J.*, to be published.

[4] Y. Xu and J. Xia, "Q-learning based physical-layer secure game against multi-agent attacks," *IEEE Access*, to be published.

[5] X. Lai, L. Fan, X. Lei, J. Li, N. Yang, and G. K. Karagiannidis, "Distributed secure switch-and-stay combining over correlated fading channels," *IEEE Trans. Inf. Forensics Security*, to be published.

[6] N. Deng and M. Haenggi, "A fine-grained analysis of millimeter-wave device-to-device networks," *IEEE Trans. Commun.*, vol. 65, no. 11, pp. 4940–4954, Nov. 2017.

[7] X. Liu, M. Jia, Z. Na, W. Lu, and F. Li, "Multi-modal cooperative spectrum sensing based on dempster-shafer fusion in 5G-based cognitive radio," *IEEE Access*, vol. 6, pp. 199–208, 2018.

[8] M. Jia, Z. Yin, Q. Guo, G. Liu, and X. Gu, "Downlink design for spectrum efficient IoT network," *IEEE Internet Things J.*, vol. 5, no. 5, pp. 3397–3404, Oct. 2018.

[9] X. Lin and J. Xia, "MARL-based distributed cache placement for wireless networks," *IEEE Access*, to be published.

[10] X. Liu, F. Li, and Z. Na, "Optimal resource allocation in simultaneous cooperative spectrum sensing and energy harvesting for multichannel cognitive radio," *IEEE Access*, vol. 5, pp. 3801–3812, 2017.

[11] J. Zhang, X. Tao, H. Wu, and X. Zhang, "Secure transmission in SWIPT-powered two-way untrusted relay networks," *IEEE Access*, vol. 6, pp. 10508–10519, 2018.

[12] X. Zhou, R. Zhang, and C. K. Ho, "Wireless information and power transfer in multiuser OFDM systems," in *Proc. IEEE Global Commun. Conf. (GLOBECOM)*, Apr. 2013, pp. 4092–4097.

[13] J. Yang, Y. Cheng, K. P. Peppas, P. T. Mathiopoulos, and J. Ding, "Outage performance of cognitive DF relaying networks employing SWIPT," *China Commun.*, vol. 15, no. 4, pp. 28–40, 2018.

[14] Y. Liu, "Joint resource allocation in SWIPT-based multiantenna decode-and-forward relay networks," *IEEE Trans. Veh. Technol.*, vol. 66, no. 10, pp. 9192–9200, Oct. 2017.

[15] M. Xia and S. Aissa, "On the efficiency of far-field wireless power transfer," *IEEE Trans. Signal Process.*, vol. 63, no. 11, pp. 2835–2847, Jun. 2015.

[16] C. Li and W. Zhou, "Enhanced secure transmission against intelligent attacks," *IEEE Access*, to be published.

[17] N. Deng and M. Haenggi, "The energy and rate meta distributions in wirelessly powered D2D networks," *IEEE J. Sel. Areas Commun.*, vol. 37, no. 2, pp. 269–282, Feb. 2019.

[18] S. H. Kim and D. I. Kim, "Performance tradeoff in two-zone based wireless powered communication networks," in *Proc. Int. Symp. Wireless Commun. Syst. (ISWCS)*, Aug. 2015, pp. 286–290.

[19] B. Lyu, Z. Yang, G. Gui, and Y. Feng, "Wireless powered communication networks assisted by backscatter communication," *IEEE Access*, vol. 5, pp. 7254–7262, 2017.

[20] B. Lyu, H. Guo, Z. Yang, and G. Gui, "Throughput maximization for hybrid backscatter assisted cognitive wireless powered radio networks," *IEEE Internet Things J.*, vol. 5, no. 3, pp. 2015–2024, Jun. 2018.

[21] Y. Liu, L. Wang, M. Elkashlan, T. Q. Duong, and A. Nallanathan, "Two-way relaying networks with wireless power transfer: Policies design and throughput analysis," in *Proc. IEEE Global Commun. Conf.*, Dec. 2014, pp. 4030–4035.

[22] Z. Na, J. Lv, F. Jiang, M. Xiong, and N. Zhao, "Joint subcarrier and subsymbol allocation based simultaneous wireless information and power transfer for multiuser GFDM in IoT," *IEEE Internet Things J.*, to be published.

[23] D. Zhang, M. Matthé, L. L. Mendes, and G. Fettweis, "A study on the link level performance of advanced multicarrier waveforms under MIMO wireless communication channels," *IEEE Trans. Wireless Commun.*, vol. 16, no. 4, pp. 2350–2365, Apr. 2017.

[24] Z. Na, M. Zhang, M. Jia, M. Xiong, and Z. Gao, "Joint uplink and downlink resource allocation for the Internet of Things," *IEEE Access*, vol. 7, pp. 15758–15766, 2019.

[25] A. E. Shafie, K. Tourki, and N. Al-Dhahir, "An artificial-noise-aided hybrid TS/PS scheme for OFDM-based SWIPT systems," *IEEE Commun. Lett.*, vol. 21, no. 3, pp. 632–635, Mar. 2017.

[26] Z. Na, X. Li, X. Liu, and Z. Deng, "Subcarrier allocation based simultaneous wireless information and power transfer for multiuser OFDM systems," *EURASIP J. Wireless Commun. Netw.*, vol. 2017, no. 1, p. 148, 2017. doi: 10.1186/s13638-017-0932-1.

[27] X. Liu, X. Zhang, M. Jia, L. Fan, W. Lu, and X. Zhai, "5G-based green broadband communication system design with simultaneous wireless information and power transfer," *Phys. Commun.*, vol. 28, pp. 130–137, Jun. 2018. [Online]. Available: http://www.sciencedirect.com/science/article/pii/S1874490718300879

[28] Z. Liu, X. Tao, and W. U. Rehman, "Resource allocation for two-way amplify and forward OFDM relay networks," *China Commun.*, vol. 14, no. 8, pp. 76–82, 2017.

[29] W. Lu, Y. Gong, X. Liu, J. Wu, and H. Peng, "Collaborative energy and information transfer in green wireless sensor networks for smart cities," *IEEE Trans. Ind. Informat.*, vol. 14, no. 4, pp. 1585–1593, Apr. 2018.

[30] Y. Zhang *et al.*, "Multi-dimensional resource optimization for incremental AF-OFDM systems with RF energy harvesting relay," *IEEE Trans. Veh. Technol.*, vol. 68, no. 1, pp. 613–627, Jan. 2019.

[31] S. Gong, X. Huang, J. Xu, W. Liu, P. Wang, and D. Niyato, "Backscatter relay communications powered by wireless energy beamforming," *IEEE Trans. Commun.*, vol. 66, no. 7, pp. 3187–3200, Jul. 2018.

[32] N. Michailow *et al.*, "Generalized frequency division multiplexing for 5th generation cellular networks," *IEEE Trans. Commun.*, vol. 62, no. 9, pp. 3045–3061, Sep. 2014.

[33] W. Lu, Y. Gong, J. Wu, H. Peng, and J. Hua, "Simultaneous wireless information and power transfer based on joint subcarrier and power allocation in OFDM systems," *IEEE Access*, vol. 5, pp. 2763–2770, 2017.

[34] W. Lu, X. Wu, Q. Li, and N. Zhang, "Secondary spectrum access based on cooperative OFDM relaying," in *Proc. IEEE 75th Veh. Technol. Conf. (VTC Spring)*, May 2012, pp. 1–5.

[35] Z. Gao and B. Wang, "User cooperation in OFDM-based cognitive radio networks with simultaneous wireless information and power transfer," in *Proc. Int. Conf. Wireless Commun. Signal Process. (WCSP)*, Oct. 2015, pp. 1–6.

[36] W. D. Lu, Y. Gong, S. H. Ting, X. L. Wu, and N. T. Zhang, "Cooperative OFDM relaying for opportunistic spectrum sharing: Protocol design and resource allocation," *IEEE Trans. Wireless Commun.*, vol. 11, no. 6, pp. 2126–2135, Jun. 2012.

[37] W. Yu and R. Lui, "Dual methods for nonconvex spectrum optimization of multicarrier systems," *IEEE Trans. Commun.*, vol. 54, no. 7, pp. 1310–1322, Jul. 2006.

ZHENYU NA received the B.S. and M.S. degrees in communication engineering from the Harbin Institute of Technology, China, in 2004 and 2007, respectively, and the Ph.D. degree in information and communication engineering from the Communication Research Center, Harbin Institute of Technology, in 2010. He is currently an Associate Professor with the School of Information Science and Technology, Dalian Maritime University, China. His research interests include satellite communications and networking, orthogonal frequency-division multiplexing, non-orthogonal multicarrier transmissions, NOMA, and wireless-powered communication networks.

JIAQI LV received the B.S. degree in electronic information science and technology from Yunnan University, Kunming, China, in 2016. She is currently pursuing the M.S. degree with the School of Information Science and Technology, Dalian Maritime University, China. Her research interests include 5G wireless communications, generalized frequency-division multiplexing, and wireless-powered communication.

MENGSHU ZHANG received the B.S. degree in communication engineering from Dalian Maritime University, Dalian, China, in 2017. She is currently pursuing the M.S. degree with the School of Information Science and Technology, Dalian Maritime University. Her research interests include 5G wireless communications, synchronization, orthogonal frequency-division multiplexing, NOMA, and satellite communication.

BAO PENG received the Ph.D. degree in information and communication engineering from the School of Electronics and Information Engineering, Harbin Institute of Technology, Harbin, China, in 2009. He is currently an Associate Professor with the School of Electronic Communication Technology, Shenzhen Institute of Information Technology. His research interests include wireless sensor networks, distributed systems, and the Internet of Things.

MUDI XIONG received the M.Sc. degree in physics electronics from the Changchun Institute of Optics and Fine Mechanics, in 1994, and the Ph.D. degree in optical engineering from Changchun Institute of Optics, Fine Mechanics and Physics, Chinese Academy of Sciences, in 2000. Before 2003, he was an Associate Professor with the Harbin Institute of Technology. In 2003, he came to Dalian Maritime University, where he has been a full-time Professor, since 2006. His research interests include optical signal detection, and optical communications and networking.

MINGXIANG GUAN received the B.S. degree in electronic engineering from the Harbin University of Science and Technology, China, in 2002, and the M.S. and Ph.D. degrees in information and communication engineering from the Harbin Institute of Technology, China, in 2004 and 2008, respectively. He is currently a full-time Professor with the School of Electronic Communication Technology, Shenzhen Institute of Information Technology. His main research interests include wireless communications, resource allocation, HAPS-based communications and networking, and HAPS-based 5G communications.